Bioorganic & Medicinal Chemistry 21 (2013) 903–911

Contents lists available at SciVerse ScienceDirect

Bioorganic & Medicinal Chemistry

journal homepage: www.elsevier.com/locate/bmc

Probing the steric requirements of the γ-aminobutyric acid aminotransferase active site with fluorinated analogues of vigabatrin

Jose I. Juncosa Jr.[a], Andrew P. Groves[a], Guoyao Xia[a], Richard B. Silverman[a,b,*]

[a] Department of Chemistry, Chemistry of Life Processes Institute, and Center for Molecular Innovation and Drug Discovery, Northwestern University, 2145 Sheridan Road, Evanston, IL 60208-3113, United States
[b] Department of Molecular Biosciences, Chemistry of Life Processes Institute, and Center for Molecular Innovation and Drug Discovery, Northwestern University, 2145 Sheridan Road, Evanston, IL 60208-3113, United States

ARTICLE INFO

Article history:
Received 31 October 2012
Revised 30 November 2012
Accepted 7 December 2012
Available online 20 December 2012

Keywords:
γ-Aminobutyric acid aminotransferase
Vigabatrin
4-Amino-5-fluoropentanoic acid
Enzyme inhibition
Molecular dynamics

ABSTRACT

We have synthesized three analogues of 4-amino-5-fluorohexanoic acids as potential inactivators of γ-aminobutyric acid aminotransferase (GABA-AT), which were designed to combine the potency of their shorter chain analogue, 4-amino-5-fluoropentanoic acid (AFPA), with the greater enzyme selectivity of the antiepileptic vigabatrin (Sabril®). Unexpectedly, these compounds failed to inactivate or inhibit the enzyme, even at high concentrations. On the basis of molecular modeling studies, we propose that the GABA-AT active site has an accessory binding pocket that accommodates the vinyl group of vigabatrin and the fluoromethyl group of AFPA, but is too narrow to support the extra width of the distal methyl group in the synthesized analogues.

1. Introduction

γ-Aminobutyric acid (GABA, **1**) is the most important inhibitory neurotransmitter in the central nervous system (CNS) of mammals. Its function as a neurotransmitter involves binding at pre- and postsynaptic receptors at inhibitory synapses in the brain. This event triggers the flow of chloride and potassium ions in and out of the cell, respectively, through specific channels. Low levels of GABA in the brain have been associated with anxiety, pain, mania, depression, and seizures, mainly due to overstimulation of other neurotransmitter receptors by their endogenous agonists.[1]

An approach that has been successfully used to treat disorders resulting from low levels of GABA in the brain, involves increasing its concentration by either stimulating its biosynthesis or inhibiting its metabolism. Vigabatrin (Sabril®, **2**), which is used in cases where classic antiepileptics are ineffective, is an example of a drug that works by the second mechanism. Vigabatrin irreversibly inhibits the chief catabolizer of GABA, γ-aminobutyric acid aminotransferase (GABA-AT), which catalyzes the transformation of GABA into succinic semialdehyde. This metabolite is later oxidized to succinate and reincorporated into the citric acid cycle.[1]

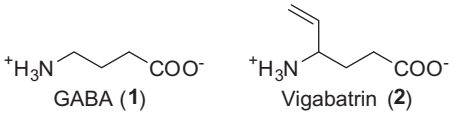

Figure 1. Structures of GABA (**1**) and vigabatrin (**2**).

Inhibition of GABA-AT by vigabatrin has been shown to involve two distinct mechanisms (Scheme 1).[2] After the formation of a Schiff base between the drug and the cofactor pyridoxal phosphate (PLP), Lys329 (the previous anchor point for the aldehyde) deprotonates the γ-proton, and tautomerizes the complex in two ways (pathways a and b). Pathway "a" creates a Michael acceptor moiety in the substrate (**3**); Lys329 undergoes 1,4-addition to give **4**. Pathway "b" involves tautomerization through the alkene, leading to enamine adduct **5**, which releases enamine **6** that reattaches to the PLP to give **7**. The observed products of the reaction were determined to be in the ratio of ~75% for the Michael addition pathway and ~25% for the enamine pathway.

Aside from its use as an antiepileptic, vigabatrin has more recently emerged as a possible novel treatment for addiction.[3–5] However, its side effect profile is detrimental to its use, especially relating to the permanent visual field defects (VFDs) induced in 25–40% of patients after chronic dosage. One explanation for the undesired side effects of vigabatrin stems from the release of a reactive metabolite. On the basis of the proposed inactivation pathways of GABA-AT by vigabatrin, one such metabolite could be the hydrolysis product of unsaturated imine **3** in the Michael addition pathway, which was shown to be generated.[2] If this is responsible for the side effects,

* Corresponding author. Tel.: +1 847 491 5653; fax: +1 847 491 7713.
E-mail address: r-silverman@northwestern.edu (R.B. Silverman).

0968-0896/$ - see front matter © 2012 Elsevier Ltd. All rights reserved.
http://dx.doi.org/10.1016/j.bmc.2012.12.009

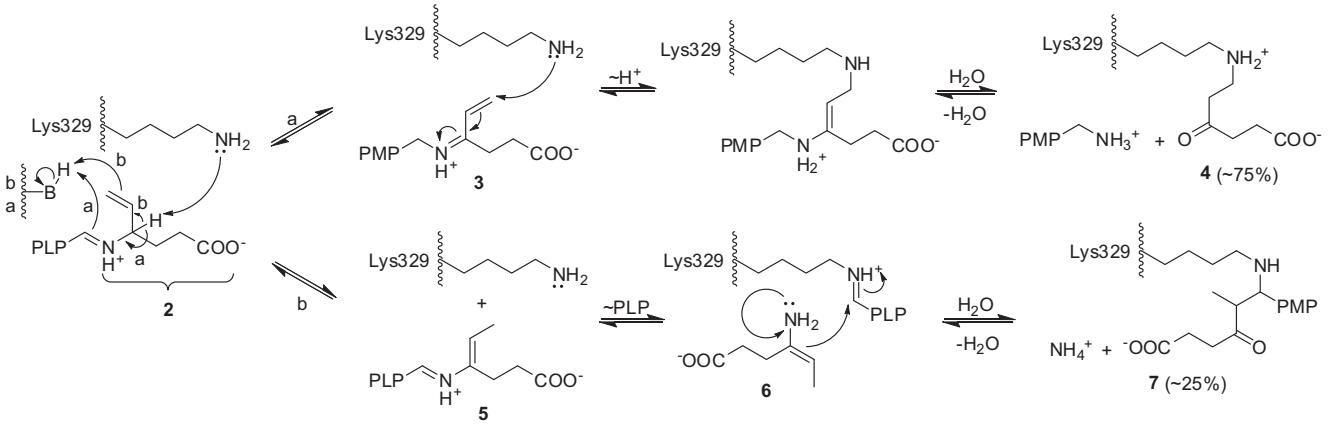

Scheme 1. Mechanisms of inactivation of GABA-AT by vigabatrin (**2**).

an approach to mitigate the VFDs caused by vigabatrin could be to bias the inactivation toward the minor enamine pathway b.

5-Fluoro-4-aminopentanoic acid (**8**) has long been known as a very efficient inactivator of GABA-AT that inhibits the enzyme exclusively through a mechanism (Scheme 2, R = H) that involves Schiff base formation with PLP followed by elimination of HF to **9** (R = H), leading only to the enamine pathway (**10**, R = H).[6] We thought we could take advantage of this mechanism by synthesizing **11** or **12**, which are identical to **8** except for the addition of a *gem*-methyl group on the carbon with the fluorine atom. However, elimination of HF from **11** or **12** would lead to the identical enamine intermediate (**5**, Scheme 1) found by tautomerization of **2**. If this occurs, then **11** or **12** would be a vigabatrin mimic that proceeds exclusively by vigabatrin's minor enamine pathway (pathway b, Scheme 1). This is depicted in Scheme 2, where R = CH_3 (compare **9**, R = CH_3 to **5** in Scheme 1).

Off-target effects of **8** are significant, especially at glutamate decarboxylase (GAD, required for GABA synthesis) and, to a lesser extent, at aspartate aminotransferase (Asp-AT).[7] Vigabatrin (**2**), which is based on a hexanoic acid skeleton, shows no activity at GAD and weakly affects Asp-AT.[8,9] We, therefore, thought that hexanoic acids **11** and/or **12** would be excellent inactivators of GABA-AT, while displaying improved enzyme selectivity when compared to their shorter chain analogue **8**.

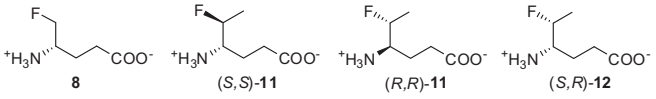

Figure 2. 4-Amino-5-fluorohexanoic acid (**8**) and the designed hexanoic acid analogues (**11** and **12**).

2. Results and discussion

2.1. Synthesis

The devised synthetic route was based around the asymmetric dihydroxylation/lactonization of a hexenoate ester and involved the use of azide as a nitrogen source, as well as a benzyl ester as a carboxylate protecting group. These choices were made to simplify the isolation and purification of the zwitterion after the final hydrogenolysis; under these conditions, only simple recrystallization was required instead of ion exchange chromatography (Scheme 3).

The synthesis of (*S,S*)-**11**, (*R,R*)-**11**, and **12**, started with the Claisen–Johnson rearrangement of 3-buten-2-ol (**13**) and triethyl orthoacetate. The continuous removal of ethanol during this reaction, which was reported to result in good yields,[10] led to the formation of product **14** along with its corresponding 3-buten-2-ol ester; this mixture was difficult to separate, and yields were low as a result. We recommend against this modification of the classic conditions.

Asymmetric dihydroxylation/lactonization of unsaturated ester **14** led to hydroxyethyl butenolide (*R,R*)-**15**, the key intermediate of this synthesis.[11] Fluorination of this compound using XtalFluor E® ((diethylamino)difluorosulfonium tetrafluoroborate) and DBU (1,8-diazabicycloundec-7-ene) yielded intermediate (*R,S*)-**16**, which was hydrolyzed under basic conditions and esterified to give acyclic fluorinated alcohol (*R,S*)-**17**.

The hydroxyl group in (*R,S*)-**17** was replaced by azide under Mitsunobu conditions using DPPA (diphenylphosphoryl azide) and DIAD (diisopropyl azodicarboxylate), and the resulting azide (*S,S*)-**18** was hydrogenated to give final compound (*S,S*)-**11**. The chiral purity of the product was determined by derivatization as the Mosher amide, and was found to have 92% ee.

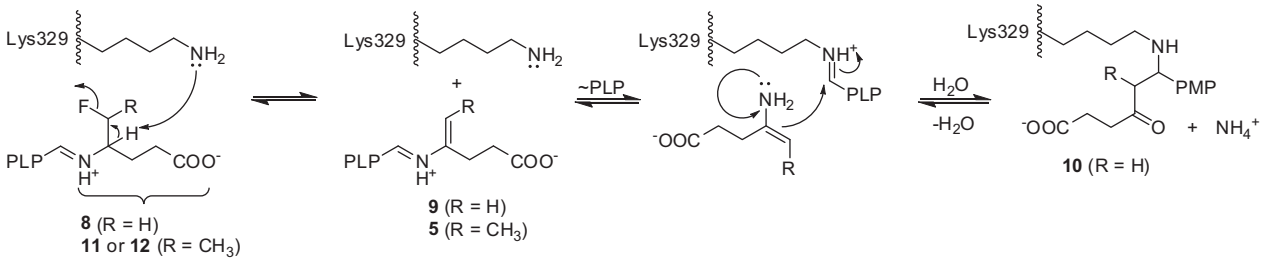

Scheme 2. Mechanism of inactivation of GABA-AT by fluorinated compounds **8**, **11**, or **12**.

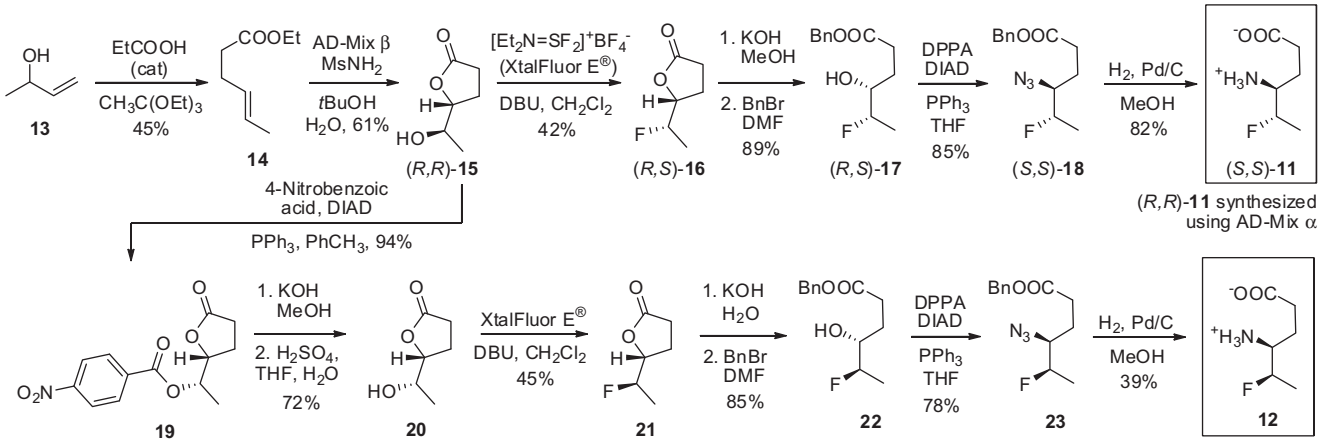

Scheme 3. Synthesis of fluorinated GABA analogues **11** and **12**.

Compound (*R,R*)-**11** was obtained in a manner similar to that of its enantiomer, but using AD-Mix α instead of its β counterpart, and DAST (diethylaminosulfur trifluoride) instead of XtalFluor E® for the fluorination step.

The synthesis of compound **12** was initially attempted through the double inversion of *ent*-**17** to give **23**. However, this strategy failed, and efforts were shifted toward the inversion of (*R,R*)-**15** via a Mitsunobu protocol. Although the reaction failed with picolinic acid,[12] the use of 4-nitrobenzoic acid was successful, as reported earlier.[11]

After subjecting diester **19** to literature conditions designed to obtain butenolide **20** exclusively (free from the competing tetrahydropyrone product),[11] we were delighted to obtain only the desired product in a good yield. Fluorination of this compound led to **21**, and the synthesis was completed as before (Scheme 3).

The enantiomer of **12** was not synthesized because it is known that active GABA compounds of this type have *S* stereochemistry at the amine carbon. Therefore, the *R* isomer was not a particularly attractive synthetic target to warrant the additional work (See Figs. 1 and 2).

2.2. Enzymatic assays

Compounds (*S,S*)-**11**, (*R,R*)-**11**, and **12** were tested for time-dependent inhibition of GABA-AT at 5 mM concentrations; vigabatrin (**2**) was used as a positive control. Unfortunately, no inactivation of the enzyme was observed by any of the synthesized molecules (Fig. 3).

Similarly, no reversible inhibition of GABA-AT was observed with any of the three compounds at 23 mM concentration (Fig. 3, bottom). In this case, reversible inhibitor **24**[13] was employed as a positive control. Consistent with these results, the compounds did not show significant substrate activity with the enzyme; at a concentration of 3 mM, (*S,S*)-**11**, (*R,R*)-**11**, and **12** showed glutamate production relative to GABA of 0.11%, 0.02% and 0.32%, respectively ($n = 2$).

2.3. Molecular modeling

In an attempt to find an explanation for the low inactivation properties of the synthesized compounds, we decided to carry out molecular modeling studies. On the basis of the published X-ray structure of GABA-AT inactivated by vigabatrin (pdb code 1OHW),[14] we performed docking studies of (*S,S*)-**11**, **8**, and vigabatrin (**2**) in the active site, followed by molecular dynamics (MD) simulations and energy minimization. Upon analyzing the binding

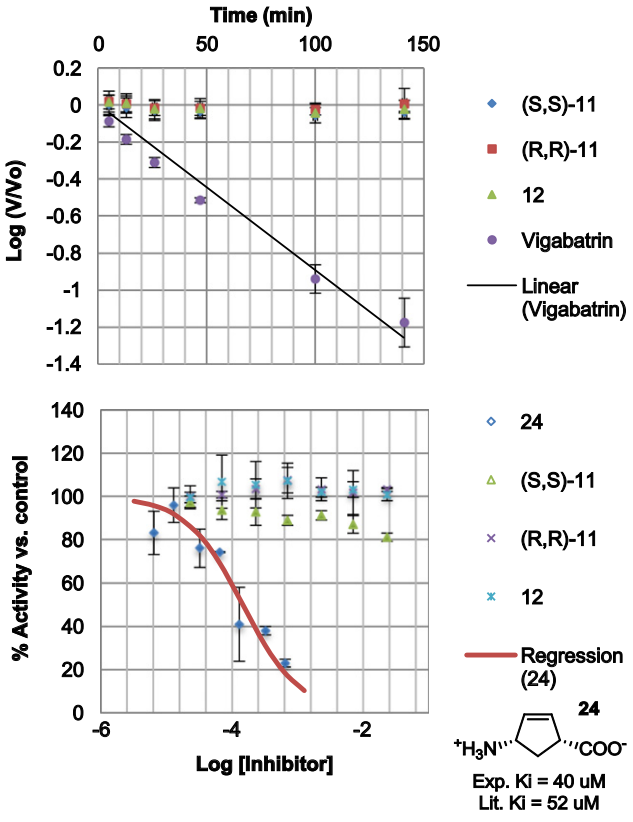

Figure 3. Top: Inactivation study of GABA-AT with (*S,S*)-**11**, (*R,R*)-**11**, **12**, and **2**. Bottom: Competitive binding of (*S,S*)-**11**, (*R,R*)-**11**, **12**, and **20**, at GABA-AT ($n = 3$ for all measurements).

of the compounds in the active site, we found that there is a small, narrow accessory binding pocket adjacent to the main cavity. This space is occupied by the terminal vinyl group when vigabatrin is bound (Fig. 4, middle); in the case of **8**, it is mostly empty.

We were surprised to see that the terminal methyl group of (*S,S*)-**11** did not occupy the same space during about a third of the simulation time; during a significant interval, it instead preferred pointing toward the access channel (Fig. 4). This occurred in spite of the resulting unfavorable *syn*-pentane interaction with carbon **2** (α to the carboxylate), which carries with it an energetic penalty of around 3.6 kcal/mol.

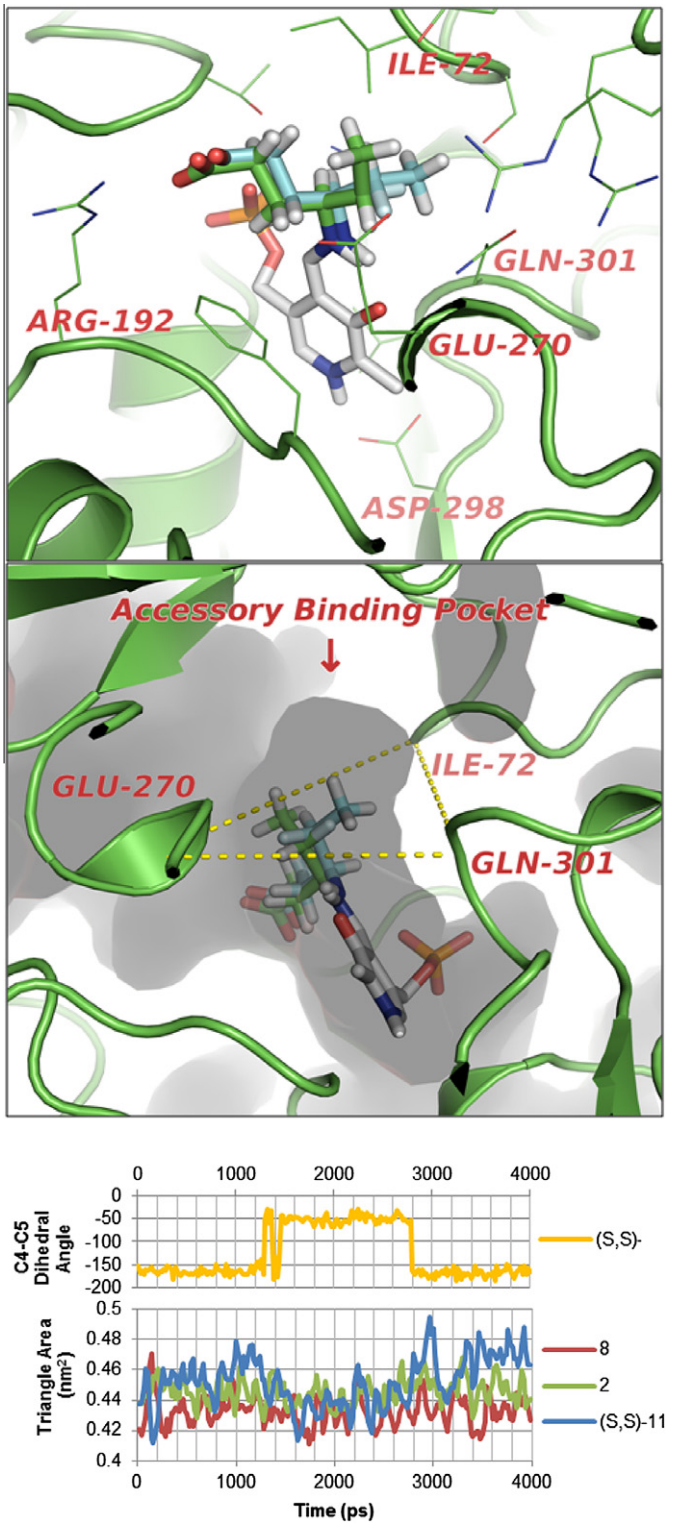

Figure 4. Top: Observed conformations of (*S,S*)-**11** within the GABA-AT binding pocket during the MD simulations. Vigabatrin adopts an orientation similar to the extended (blue) conformer. PLP is shown in gray. Middle: Location of (*S,S*)-**11** relative to the active site surface; yellow: triangle used to track the width of the accessory binding pocket during MD. Bottom (during MD time frame, averaged over three values for smoothing): Yellow: C4-C5 dihedral angle for (*S,S*)-**11**; Red, green, and blue: Area of yellow triangle in middle panel during the simulations with compounds **8**, **2**, and (*S,S*)-**11**, respectively.

Because the starting pose of the compound was analogous to that of vigabatrin in the inactivated enzyme complex, that is, with the methyl group in the vicinity of the accessory pocket, we were intrigued by the conformational shift that occurred during the MD simulation. We analyzed the evolution of the relevant dihedral angle during the simulation, and found that there had, in fact, been a shift from the *anti* to the *gauche* conformation and back to anti toward the end of the simulation (Fig. 4, bottom).

We propose that the reason for these conformational shifts is the narrow width of the accessory-binding pocket. As a planar substituent, the vinyl group of vigabatrin is narrower than the distal methyl group of (*S,S*)-**11** and is accommodated by the available space. However, the methyl group is apparently too wide to fit into the pocket without incurring steric penalties. As a crude measure of the width of the binding pocket, we have calculated the area of the triangle formed by the Cα of Ile72, Glu270, and Gln301, at regular time intervals. The results can be seen in Figure 4 (bottom). In the case of **8**, the area has an average of 43.3 ± 0.01 Å^2, which can be taken as the unoccupied width. When vigabatrin is bound, the pocket is slightly widened at 44.6 ± 0.01 Å^2, owing to the alkene substituent; this substituent appears to be well tolerated. However, for (*S,S*)-**11**, the width goes from 45.3 ± 0.02 Å^2 when occupied back to 43.8 ± 0.02 Å^2 when empty, and then is again expanded to the even wider 46.7 ± 0.03 Å^2 after returning to the original conformation.

The observed conformational transitions for the proposed inactivator lead us to believe that adopting the extended *anti* conformation, with the terminal methyl group residing in the accessory-binding pocket, incurs an energetic penalty in the vicinity of the aforementioned 3.6 kcal/mol. We attribute this to the cost of expanding the accessory-binding pocket. In other words, both of the two possible conformations of the compound in the active site are substantially higher in energy than those for **2** or **8**. We believe this occurrence explains the lack of binding affinity of **11** and **12** for GABA-AT, and thus, their inefficacy as inactivators.

3. Conclusions

We synthesized a series of 4-amino-5-fluorohexanoic acids (both enantiomers of **11** and **12**) as potential inactivators of GABA-AT. The rationale behind these compounds was that adding an extra carbon to enamine-pathway inactivator **8**, such as the one in vigabatrin, would improve its selectivity over other enzymes. Unfortunately, the compounds were shown not to inactivate or competitively inhibit GABA-AT. After carrying out molecular modeling studies, we found that there exists an accessory-binding pocket adjacent to the main active site of the enzyme, which accommodates the flat vinyl group of vigabatrin. For (*S,S*)-**11**, the corresponding methyl group appears to be too voluminous to fit in the cavity, causing unfavorable steric interactions with the protein; an alternative conformation was observed, but a steric clash occurred as well, in this case intramolecularly. Understanding the topology of this accessory-binding pocket will allow us to refine our inactivator design process, with the goal of achieving improved enamine pathway GABA-AT inactivators, with good selectivity for the enzyme.

4. Experimental section

4.1. Materials and methods

^{1}H NMR and ^{13}C NMR spectra were recorded on a Bruker Avance III 500 MHz spectrometer. ^{19}F NMR spectra were obtained on an Agilent DDR2 400 MHz spectrometer. Chemical shifts for are reported as δ values in ppm relative to tetramethylsilane (^{1}H, ^{13}C) or $CFCl_3$ (^{19}F), with the $CHCl_3$ signal arbitrarily set as 7.27 (^{1}H) or 77.0 (^{13}C) ppm. Melting points were determined in a Büchi B540 melting point apparatus using open capillary tubes, and are uncorrected. Mass spectra were obtained with a Thermo Finnigan LCQ

electrospray impact low resolution mass spectrometer, or an Agilent LC-TOF 6210 (accurate mass), using 1:1 dichloromethane/methanol as an eluent. Optical rotations were measured in an Optical Activity Limited AA-100 polarimeter, using a 0.5 dm, 1.3 mL cell. Column chromatography was performed with Sorbent Technologies silica gel, (60 Å pore size, 230 × 400 mesh) or on an Agilent 971-FP machine using pre-packed 50 μ silica columns (Analogix, Silicycle, or Agilent). Thin layer chromatography was carried out using Baker-Flex® plastic-backed plates coated with silica gel IB2 and fluorescent indicator. Purity was determined on an Agilent 1260 reverse phase analytical HPLC, using evaporative light scattering detection (Agilent 385 ELSD); a C18 column (Gemini® 5 μm NX, 110 Å pore size, 50 × 4.6 mm size) was used with 5% acetonitrile in water (0.05% TFA) as the mobile phase (0.8 mL/min).

All reagents were purchased from Aldrich, and were used as received, except when noted. Solvents were dried using cartridge-filled drying trains.

NMR spectra were analyzed with the help of MNova 7 (MestreLab Research, Santiago de Compostela, Spain, http://mestrelab.com).

4.2. Synthetic procedures and characterization

4.2.1. (*E*)-Ethyl hex-4-enoate (14)

Neat propionic acid (126.2 μL, 125.2 mg, 1.681 mmol) was added to a mixture of 3-buten-2-ol (25.00 g, 336.3 mmol) and triethyl orthoacetate (100 mL, 86.73 g, 534.6 mmol) in a 3-necked flask fitted with a reflux condenser over a liquid addition funnel. The magnetically stirred solution was heated to 135 °C under nitrogen. Every 2 h, the funnel was closed and a sample of the condensate was analyzed by NMR. When no more starting alcohol was found in the distillate, the reaction was brought to room temperature and water (30 mL) was added. Stirring was continued for 30 min, and the low-boiling components were distilled off with minimal vacuum, using an additional 30 mL ethanol to remove residual water. Then, a higher vacuum was applied to distill the product. Column chromatography (20% dichloromethane in hexanes) led to the product (21.535 g, 151.44 mmol, 45%) as a clear, volatile liquid, and significant amounts of 3-buten-2-yl hex-4-enoate as a side product (yield not determined). ^{1}H NMR (500 MHz, $CDCl_3$) δ (ppm) 5.56–5.36 (2H, m, =CH), 4.12 (2H, q, J = 7.1 Hz, OCH_2), 2.38–2.32 (2H, m, C=CCH_2), 2.32–2.26 (2H, m, O=CCH_2), 1.64 (3H, dq, J = 6.1, 1.2 Hz, C=CCH_3), 1.25 (3H, t, J = 7.1 Hz, OCH_2CH_3); ^{13}C NMR (125 MHz, $CDCl_3$) δ (ppm) 173.25, 129.16, 126.07, 60.19, 34.30, 27.89, 17.85, 14.21.

4.2.2. (*R*)-5-((*R*)-1-Hydroxyethyl)dihydrofuran-2(3*H*)-one ((*R*,*R*)-15)

To a vigorously stirred mixture of AD-mix[15] β (26.61 g, Sigma–Aldrich) and methanesulfonamide (1.864 g, 19.01 mmol) in *t*-BuOH/H_2O (1:1, 100 mL) at 4 °C, was added unsaturated ester **14** (3.00 mL, 2.703 g, 19.01 mmol). Stirring was continued at that temperature for 4 days. At this point, the reaction was complete by TLC (1:1 EtOAc/hexanes) and solid $NaHSO_3$ (30 g) was added. After stirring for another 1 h, the suspension had turned white and was partitioned between water and ethyl acetate (50 mL each). The aqueous phase was then extracted with ethyl acetate (3 × 50 mL), and the combined organic fractions were dried (Na_2SO_4), filtered, and the solvent removed. The crude was subjected to column chromatography (20% EtOAc in hexanes and 0–5% MeOH in CH_2Cl_2), leading to the product (1.506 g, 11.57 mmol, 61%) as a clear oil. $[\alpha]^{25}$ −46° (c = 0.49, $CHCl_3$); ^{1}H NMR (500 MHz, $CDCl_3$) δ (ppm) 4.35 (1H, td, J = 7.4, 5.4 Hz, COOCH), 3.79 (1H, p, J = 6.3 Hz, HOCH), 2.66–2.52 (2H, m, CH_2COO), 2.27 (1H, dddd, J = 12.5, 9.5, 7.3, 5.0 Hz, CH_2CH_2COO), 2.19 (1H, br s, OH), 2.05 (1H, dddd, J = 12.9, 9.9, 9.1, 7.6 Hz, CH_2CH_2COO), 1.27 (3H, d, J = 6.5 Hz, CH_3); ^{13}C NMR (125 MHz, $CDCl_3$) δ (ppm) 177.29, 84.23, 69.82, 28.68, 24.03, 18.45; ESI-MS (m/z, abundance): 261 (100, $[2\,M+H]^+$), 131 (56, $[M+H]^+$).

4.2.3. (*S*)-5-((*S*)-1-Hydroxyethyl)dihydrofuran-2(3*H*)-one ((*S*,*S*)-15)

This was synthesized similarly to (*R*,*R*)-**15**, but using AD-Mix α. From 5.079 g (35.71 mmol) of ester **10**, 3.011 g (23.14 mmol, 65%) of product were obtained. $[\alpha]^{25}$ +46° (c = 0.49, $CHCl_3$); all other spectral data were similar to (*R*,*R*)-**15**.

4.2.4. (*R*)-5-((*S*)-1-Fluoroethyl)dihydrofuran-2(3*H*)-one ((*R*,*S*)-16)

To a solution of alcohol (*R*,*R*)-**15** (0.4073 g, 3.130 mmol) in CH_2Cl_2 (10 mL) at −78 °C was added DBU (716 μL, 0.729 mg, 4.69 mmol), followed by XtalFluor-E® ((diethylamino)difluorosulfonium tetrafluoroborate) (1.075 g, 4.695 mmol). After 30 min, the reaction was allowed to reach room temperature, and stirring was continued for 24 h. Then, 5% aqueous $NaHCO_3$ (10 mL) was added, and after stirring another 15 min, the aqueous layer was extracted with CH_2Cl_2 (2 × 10 mL). The combined organic phases were dried ($MgSO_4$), filtered through a pad of silica gel with abundant CH_2Cl_2, and the solvent was removed. Column chromatography (10–30% ethyl acetate in hexanes) gave the product (0.1721 g, 1.303 mmol, 42%) as a clear oil. $[\alpha]^{25}$ +2° (c = 0.44, $CHCl_3$); ^{1}H NMR (500 MHz, $CDCl_3$) δ (ppm) 4.84 (1H, dqd, J = 48.7, 6.5, 3.4 Hz, CHF), 4.46 (1H, dddd, J = 20.9, 7.9, 6.0, 3.4 Hz, CHO), 2.69–2.45 (2H, m, CH_2COO), 2.40–2.17 (2H, m, CH_2CH_2COO), 1.38 (3H, dd, J = 23.7, 6.6 Hz, CH_3); ^{13}C NMR (126 MHz, $CDCl_3$) δ (ppm) 176.59, 89.75 (d, J = 173.4 Hz), 80.97 (d, J = 23.4 Hz), 27.88, 21.61 (d, J = 4.8 Hz), 16.50 (d, J = 22.1 Hz); ^{19}F NMR (376 MHz, $CDCl_3$) δ (ppm) −191.6 (1F, dp, J = 23.0, 46.9 Hz); ESI-MS (m/z, abundance): 287 (93, $[2\,M+Na]^+$).

4.2.5. (*S*)-5-((*R*)-1-Fluoroethyl)dihydrofuran-2(3*H*)-one ((*S*,*R*)-16)

To a solution of alcohol (*S*,*S*)-**15** (1.859 g, 14.29 mmol) in dichloromethane (15 mL) at 0 °C, was added DAST (2.37 mL, 2.91 g, 17.1 mmol) dropwise. The reaction was allowed to reach room temperature over 16 h with magnetic stirring. Again at 0 °C, saturated aqueous $NaHCO_3$ (15 mL) was added slowly, and the mixture was extracted with dichloromethane (3 × 15 mL). The combined organic extracts were dried ($MgSO_4$), the solvent removed, and the crude subjected to column chromatography (10–30% ethyl acetate in hexanes), giving the product (0.4959 g, 1.888 mmol, 26%) as a clear oil. $[\alpha]^{25}$ −5° (c = 0.45, $CHCl_3$); all other spectral data were similar to those of (*R*,*S*)-**16**.

4.2.6. (4*R*,5*S*)-Benzyl 5-fluoro-4-hydroxyhexanoate ((*R*,*S*)-17)

To a solution of lactone (*R*,*S*)-**16** (0.1557 g, 1.178 mmol in MeOH (5 mL) was added solid KOH (0.0777 g, 1.25 mmol), and the reaction was stirred at room temperature for 16 h. The solvent was then evaporated under reduced pressure; then the solid was redissolved in DMF (5 mL) and treated with benzyl bromide (0.143 mL, 0.206 g, 1.18 mmol) dropwise. After another 16 h of stirring, the reaction was diluted with water (10 mL) and extracted with Et_2O (3 x 10 mL). The organic extracts were washed with water (2 × 5 mL), dried (Na_2SO_4), and concentrated under reduced pressure. Column chromatography (10–40% ethyl acetate in hexanes) yielded the product (0.2522 g, 1.050 mmol, 89%) as a clear oil. $[\alpha]^{25}$ +24° (c = 0.40, $CHCl_3$); ^{1}H NMR (500 MHz, $CDCl_3$) δ (ppm) 7.44–7.28 (5H, m, ArH), 5.14 (2H, s, $ArCH_2$), 4.59 (1H, dqd, J = 47.3, 6.4, 4.1 Hz, CHF), 3.80–3.64 (1H, m, HOCH), 2.69–2.46 (2H, m, CH_2COO), 2.26 (1H, s, OH), 1.90 (1H, dtd, J = 14.6, 7.4, 2.8 Hz, CH_2CH_2COO), 1.72 (1H, ddt, J = 14.0, 9.9, 6.8 Hz, CH_2CH_2COO), 1.34 (3H, dd, J = 24.8, 6.3 Hz, CH_3); ^{13}C NMR

(126 MHz, $CDCl_3$) δ (ppm) 173.81, 135.72, 128.58, 128.30, 128.25, 92.54 (d, J = 167.7 Hz), 72.84 (d, J = 22.0 Hz), 66.51, 30.65, 26.45 (d, J = 6.0 Hz), 15.38 (d, J = 22.6 Hz); ^{19}F NMR (376 MHz, $CDCl_3$) δ (ppm) −181.53 (1F, dqd, J = 48.0, 24.1, 17.9 Hz); ESI-MS (m/z, abundance): 263 (59, $[M+Na]^+$), 480 (43, $[2\ M]^+$).

4.2.7. (4*S*,5*R*)-Benzyl 5-fluoro-4-hydroxyhexanoate ((*S*,*R*)-17)

This was synthesized by the same method as that for (*R*,*S*)-**17** from lactone (*S*,*R*)-**16** (0.4463 g, 3.378 mmol), obtaining the product (0.7403 g, 3.081 mmol, 91%) as a clear oil. $[\alpha]^{25}$ −16° (c = 0.64, $CHCl_3$); all other spectral data were similar to (*R*,*S*)-**17**.

4.2.8. (4*S*,5*S*)-Benzyl 4-azido-5-fluorohexanoate ((*S*,*S*)-18)

DIAD (0.200 mL, 0.205 g, 0.964 mmol) was slowly added to a stirred solution of alcohol (*R*,*S*)-**17** (0.1931 g, 0.8037 mmol), triphenylphosphine (0.2555 g, 0.9644 mmol), and diisopropylethylamine (0.140 mL, 0.104 g, 0.804 mmol) in THF (5 mL) at 10 °C, and stirring was continued for 15 min. Diphenylphosphoryl azide (0.214 mL, 0.274 g, 0.964 mmol) was then added slowly at −15 °C, and the reaction was allowed to reach room temperature overnight. The solvent was removed under reduced pressure, and the crude product was directly subjected to column chromatography (dichloromethane) to give the product (0.1742 g, 0.6747 mmol, 85%) as a clear oil. $[\alpha]^{25}$ −20° (c = 0.29, $CHCl_3$); ^{1}H NMR (500 MHz, $CDCl_3$) δ (ppm) δ 7.47–7.25 (5H, m, ArH), 5.15 (2H, ABq, $\Delta\nu_{AB}$ = 7.28 Hz, J_{AB} = 12.3 Hz, $ArCH_2$), 4.65 (1H, dqd, J = 47.4, 6.3, 5.2 Hz, CHF), 3.34 (1H, dddd, J = 18.2, 10.3, 5.2, 3.8 Hz, CHN_3), 2.66–2.44 (2H, m, CH_2COO), 1.94 (1H, dtd, J = 14.3, 7.8, 3.9 Hz, CH_2CH_2COO), 1.80 (1H, dddd, J = 14.2, 10.3, 7.4, 6.2 Hz, CH_2CH_2COO), 1.41 (3H, dd, J = 24.2, 6.3 Hz, CH_3); ^{13}C NMR (126 MHz, $CDCl_3$) δ (ppm) 172.46, 135.64, 128.61, 128.37, 128.30, 92.22 (d, J = 173.2 Hz), 66.55, 64.69 (d, J = 19.2 Hz), 30.46, 25.22 (d, J = 5.2 Hz), 17.77 (d, J = 22.7 Hz); ^{19}F NMR (376 MHz, $CDCl_3$) δ (ppm) −181.54 (dqd, J = 48.3, 24.3, 18.1 Hz); ESI-MS (m/z, abundance): 312 (40, $[M+H+EtOH]^+$), 298 (10, $[M+H+MeOH]^+$).

4.2.9. (4*R*,5*R*)-Benzyl 4-azido-5-fluorohexanoate ((*R*,*R*)-18)

This compound was obtained through the procedure used for (*S*,*S*)-**18**, starting from (*S*,*R*)-**17** (0.2008 g, 0.8357 mmol), and yielding the product (0.1898 g, 0.7155 mmol, 86%) as a clear oil. $[\alpha]^{25}$ +23° (c = 0.34, $CHCl_3$); all other spectral data were similar to (*S*,*S*)-**18**.

4.2.10. (4*S*,5*S*)-4-Ammonio-5-fluorohexanoate ((*S*,*S*)-11)

Azido ester (*S*,*S*)-**18** (0.1414 g, 0.5330 mmol) was dissolved in methanol (12 mL) and 10% Pd/C (27 mg, 0.025 mmol) was added. The flask was flushed under vacuum and filled with hydrogen three times. A hydrogen-filled balloon was fitted to the sealed flask through a needle, and stirring was continued for 24 h at room temperature. At that time, the suspension was filtered through a pad of Celite with additional methanol (50 mL). Solvent and volatiles were removed from the filtrate under high vacuum. The crude product was recrystallized from methanol and diethyl ether to give the product (64.9 mg, 0.435 mmol, 82%) as a white solid, mp. 135–137 °C, $[\alpha]^{25}$ +41° (c = 0.36, MeOH); ^{1}H NMR (500 MHz, CD_3OD) δ (ppm) 4.76 (1H, dp, J = 48.0, 6.4 Hz, CHF), 3.30–3.17 (1H, m, CHN), 2.58–2.35 (2H, m, CH_2COO), 1.97–1.74 (2H, m, CH_2CH_2COO), 1.47 (3H, dd, J = 24.7, 6.3 Hz, CH_3); ^{13}C NMR (126 MHz, CD_3OD) δ (ppm) 181.45, 92.21 (d, J = 170.8 Hz), 58.43 (d, J = 18.4 Hz), 36.44, 27.78 (d, J = 4.9 Hz), 18.75 (d, J = 22.1 Hz); ^{19}F NMR (376 MHz, CD_3OD) δ (ppm) −182.91 (1F, dqd, J = 49.0, 24.6, 14.3 Hz); HRMS (ESI) (m/z): 150.0927 (calc, for $C_6H_{13}FNO_2^+$: 150.0925, $[M+H]^+$); ee = 92% (from Mosher amide de); HPLC purity (retention time): 95% (0.784 min).

4.2.11. (4*S*,5*S*)-5-Fluoro-4-((*S*)-3,3,3-trifluoro-2-methoxy-2-phenylpropanamido)hexanoic acid

(*R*)-(−)-α-Methoxy-α-(trifluoromethyl)phenylacetyl chloride (7.4 μL, 9.9 mg, 39 μmol) was added to a magnetically stirred solution of amine (*S*,*S*)-**11** (5.8 mg, 39 μmol) and $NaHCO_3$ (98 mg, 1.2 mmol) in water and acetone (1.5 mL each). After stirring overnight at room temperature, the mixture was evaporated under reduced pressure, and 3 M aqueous HCl (3 mL) was added. Extraction with CH_2Cl_2 (2 × 3 mL) and $CHCl_3$ (3 mL), followed by drying (Na_2SO_4), filtration, and evaporation gave the product (14.2 mg, 38.9 μmol, 100%) as a clear oil, $[\alpha]^{25}$ −11° (c = 0.25, $CHCl_3$); ^{1}H NMR (500 MHz, $CDCl_3$) δ (ppm) 7.61–7.48 (2H, m, ArH), 7.45–7.40 (3H, m, ArH), 6.99 (1H, d, J = 9.7 Hz, NH), 4.78 (1H, dqd, J = 46.9, 6.3, 1.8 Hz, CHF), 4.10 (1H, dtdd, J = 26.7, 9.7, 4.7, 1.7 Hz, CHNH), 3.57 (1H, br s, COOH), 3.45 (3H, q, J = 1.6 Hz, OCH_3), 2.39–2.27 (2H, m, CH_2COOH), 2.03–1.88 (2H, m, CH_2CH_2COOH), 1.36 (3H, dd, J = 24.4, 6.3 Hz, $CHFCH_3$); ^{13}C NMR (126 MHz, $CDCl_3$) δ (ppm) 177.67, 167.04, 132.16, 129.61, 128.71, 127.41, 123.64 (q, J = 290.2 Hz), 91.34 (d, J = 171.3 Hz), 84.03 (q, J = 26.4 Hz), 55.07, 52.04 (d, J = 18.5 Hz), 30.12, 26.97 (d, J = 3.2 Hz), 17.70 (d, J = 22.6 Hz); ^{19}F NMR (376 MHz, $CDCl_3$) δ (ppm) −69.07 (3F, s, CF_3), −189.97 (1F, ddq, J = 48.5, 27.6, 24.4 Hz, CHF); de = 92% based on CF_3 peak (3.00 F at −69.07 ppm vs 0.13 F at −69.24 ppm); (ESI-MS (m/z, abundance): 366 (100, $[M+H]^+$), 388 (23, $[M+Na]^+$), 753 (53, $[2M+Na]^+$).

4.2.12. (4*R*,5*R*)-4-Ammonio-5-fluorohexanoate ((*R*,*R*)-11)

Using the same procedure as that for (*S*,*S*)-**11**, azide (*R*,*R*)-**18** (0.1658 g, 0.6250 mmol) yielded the product (78.3 mg, 0.5249 mmol, 84%) as a white powder, mp. 131–132 °C, $[\alpha]^{25}$ −44° (c = 0.22, CD_3OD); HRMS (ESI) (m/z): 150.0926 (calc, for $C_6H_{13}FNO_2^+$: 150.0925, $[M+H]^+$); ee = 84% (from Mosher amide de); all other spectral data were similar to (*S*,*S*)-**11**. HPLC purity (retention time): 94% (0.790 min).

4.2.13. (4*R*,5*R*)-5-Fluoro-4-((*S*)-3,3,3-trifluoro-2-methoxy-2-phenylpropanamido)hexanoic acid

This compound was prepared exactly as the derivative of product (*S*,*S*)-**11**, but using amine (*R*,*R*)-**7** (5.6 mg, 38 μmol) and giving the product (13.2 mg, 36.1 μmol, 96%) as a clear oil, contaminated with (*S*)-Mosher's acid (3.1 mg, 13.2 μmol); $[\alpha]^{25}$ +8.3° (c = 0.96, $CHCl_3$), Corrected for Mosher's acid: $[\alpha]^{25}$ +27° (c = 0.78, $CHCl_3$); ^{1}H NMR (500 MHz, $CDCl_3$) δ (ppm) 7.62–7.48 (2H, m, ArH), 7.48–7.36 (3H, m, ArH), 7.08 (1H, d, J = 9.8 Hz, NH), 4.75 (1H, dqd, J = 46.9, 6.3, 2.2 Hz, CHF), 4.10 (1H, dtdd, J = 26.7, 9.5, 5.3, 2.0 Hz, CHNH), 3.57 (1H, br s, COOH), 3.39 (3H, d, J = 1.5 Hz, OCH_3), 2.54–2.40 (2H, m, CH_2COOH), 2.07–1.92 (2H, m, CH_2CH_2COOH), 1.25 (3H, dd, J = 24.4, 6.3 Hz, $CHFCH_3$); ^{13}C NMR (126 MHz, $CDCl_3$) δ (ppm) 178.05, 167.02, 131.83, 129.60, 128.71, 127.62, 123.73 (q, J = 290.3 Hz), 91.43 (d, J = 171.3 Hz), 84.06 (q, J = 26.5 Hz), 54.91, 52.14 (d, J = 18.5 Hz), 30.08, 27.02 (d, J = 3.2 Hz), 17.84 (d, J = 22.6 Hz); ^{19}F NMR (376 MHz, $CDCl_3$) δ (ppm) −69.22 (3F, s, CF_3), −189.56 (1F, ddq, J = 48.5, 27.0, 24.5 Hz, CHF); de = 84% based on CF_3 peak (3.00 F at −69.22 ppm vs 0.27 F at −69.04 ppm); (ESI-MS (m/z, abundance): 729 (100, $[2M-H]^-$), 364 (12, $[M-H]^-$).

4.2.14. (*S*)-1-((*R*)-5-Oxotetrahydrofuran-2-yl)ethyl 4-nitrobenzoate (19)

A magnetically-stirred suspension of alcohol (*R*,*R*)-**15** (0.4981 g, 3.827 mmol), triphenylphosphine (1.318 g, 4.976 mmol), and 4-nitrobenzoic acid (0.8485 g, 4.976 mmol) in toluene (10 mL) at 0 °C and under nitrogen, was treated dropwise with neat diisopropyl azodicarboxylate (1.1 mL, 1.1 g, 5.0 mmol). The reaction was allowed to reach room temperature overnight, and the solids were removed using a plug of cotton, washing with an additional

10 mL of toluene. The crystalline product was redissolved with ethyl acetate (10 mL) and the solvent was removed. The toluene solution was also evaporated under reduced pressure, and the resulting crude product was subjected to column chromatography (20–50% ethyl acetate in hexanes), giving the product as a white solid (total yield: 1.005 g, 3.599 mmol, 94%), mp: 136–138 °C, $[\alpha]^{25}$ +16° (c = 0.66, $CHCl_3$); ^1H NMR (500 MHz, $CDCl_3$) δ (ppm) 8.30 and 8.18 (4H, AA'XX', J_{AX} = 8.9 Hz, ArH), 5.39 (1H, qd, J = 6.5, 4.0 Hz, ArCOOCH), 4.69 (1H, td, J = 7.4, 4.0 Hz, lactone COOCH), 2.71–2.55 (2H, m, CH_2COO), 2.42 (1H, dddd, J = 13.5, 9.0, 7.6, 6.1 Hz, CH_2CH_2COO), 2.30–2.14 (1H, m, CH_2CH_2COO), 1.45 (3H, d, J = 6.5 Hz, CH_3).; ^{13}C NMR (126 MHz, $CDCl_3$) δ (ppm) 176.24, 163.79, 150.64, 135.13, 130.71, 123.63, 80.54, 72.16, 28.02, 23.00, 14.99; ESI-MS (m/z, abundance): 581 (100, $[2M+Na]^+$), 302 (24, $[M+Na]^+$), 280 (14, $[M+H]^+$).

4.2.15. (*R*)-5-((*S*)-1-Hydroxyethyl)dihydrofuran-2(3*H*)-one (20)

Diester **19** (0.9751 g, 3.492 mmol) was dissolved in EtOH (15 mL) at room temperature, and KOH (1.350 g, 21.65 mmol) was added. The reaction was stirred at 60 °C for 2 h, and, after cooling back to room temperature, the solvent was removed under reduced pressure. The residue was redissolved in THF and H_2O (25 mL each), and H_2SO_4 (2.3 mL, 4.2 g, 43 mmol) was added slowly. After stirring at room temperature for 24 h, the reaction was extracted with ethyl acetate (3 × 50 mL), and the combined extracts were dried (Na_2SO_4) and the solvent was removed. Column chromatography (30–50% ethyl acetate in hexanes) gave the product (0.3272 g, 2.514 mmol, 72%) as a clear oil. $[\alpha]^{25}$ −11° (c = 0.31, $CHCl_3$); ^1H NMR (500 MHz, $CDCl_3$) δ (ppm): 4.42 (1H, td, J = 7.4, 3.3 Hz, COOCH), 4.14 (1H, qd, J = 6.7, 3.4 Hz, CHOH), 2.68–2.48 (2H, m, CH_2COO), 2.35–2.12 (2H, m, CH_2CH_2COO), 2.04 (1H, br s, OH), 1.20 (3H, d, J = 6.5 Hz, CH_3); ^{13}C NMR (126 MHz, $CDCl_3$) δ (ppm) 177.36, 83.37, 67.33, 28.62, 20.93, 17.64; ESI-MS (m/z, abundance): 283 (100, $[2M+Na]^+$), 153 (34, $[M+Na]^+$), 131 (34, $[M+H]^+$).

4.2.16. (*R*)-5-((*R*)-1-Fluoroethyl)dihydrofuran-2(3*H*)-one (21)

This was prepared as detailed for (*R*,*S*)-**16**, from lactone **20** (0.3167 g, 2.434 mmol), yielding the product (0.1162 g, 0.8794 mmol, 45%) as a clear oil. $[\alpha]^{25}$ −31° (c = 0.26, $CHCl_3$); ^1H NMR (500 MHz, $CDCl_3$) δ (ppm): 4.68 (1H, dqd, J = 46.9, 6.5, 3.1 Hz, CHF), 4.49 (1H, dddd, J = 24.0, 8.1, 5.9, 3.1 Hz, $CH_3CHFCHO$), 2.64 (1H, dddd, J = 18.3, 10.1, 6.6, 1.7 Hz, CH_2COO), 2.52 (1H, dddd, J = 18.0, 10.0, 7.0, 1.5 Hz, CH_2COO), 2.34 (1H, dddd, J = 12.9, 10.0, 8.0, 6.6 Hz, CH_2CH_2COO), 2.20 (1H, dddd, J = 13.0, 10.1, 7.0, 5.9 Hz, CH_2CH_2COO), 1.45 (3H, dd, J = 23.9, 6.5 Hz, CH_3); ^{13}C NMR (126 MHz, $CDCl_3$) δ (ppm) 176.74, 90.55 (d, J = 174.9 Hz), 80.71 (d, J = 19.7 Hz), 27.95, 23.57 (d, J = 4.7 Hz), 16.63 (d, J = 23.1 Hz); ^{19}F NMR (376 MHz, $CDCl_3$) δ (ppm) −190.34 (1F, dp, J = 47.6, 23.9 Hz); ESI-MS (m/z, abundance): 568 (100, $[4M+K]^+$).

4.2.17. (4*R*,5*R*)-Benzyl 5-fluoro-4-hydroxyhexanoate (22)

This was obtained similarly to (*R*,*S*)-**17**, from lactone **21** (0.1032 g, 0.7810 mmol), giving the desired ester (0.1597 g, 0.6647 mmol, 85%) as a clear oil, $[\alpha]^{25}$ +14° (c = 0.18, $CHCl_3$); ^1H NMR (500 MHz, $CDCl_3$) δ (ppm): 7.42–7.28 (5H, m, ArH), 5.14 (2H, ABq, $\Delta\nu_{AB}$ = 6.37 Hz, J_{AB} = 12.3 Hz, $ArCH_2$), 4.51 (1H, dqd, J = 48.4, 6.3, 5.3 Hz, CHF), 3.58 (1H, ddtd, J = 16.8, 10.3, 5.3, 3.3 Hz, CHOH), 2.66–2.52 (2H, m, CH_2COO), 2.22 (1H, dd, J = 5.3, 2.2 Hz, OH), 1.94–1.71 (2H, m, CH_2CH_2COO), 1.35 (3H, dd, J = 24.7, 6.4 Hz, CH_3); ^{13}C NMR (126 MHz, $CDCl_3$) δ (ppm) 173.53, 135.80, 93.06 (d, J = 167.2 Hz), 73.34 (d, J = 19.9 Hz), 66.41, 30.27, 27.41 (d, J = 5.4 Hz), 16.92 (d, J = 22.6 Hz); ^{19}F NMR (376 MHz, $CDCl_3$) δ (ppm) −186.53 (1F, dqd, J = 49.5, 24.2, 16.6 Hz); ESI-MS (m/z, abundance): 503 (100, $[2M+Na]^+$), 264 (40, $[M+Na]^+$), 241 (23, $[M+H]^+$).

4.2.18. (4*S*,5*R*)-Benzyl 4-azido-5-fluorohexanoate (23)

This was obtained similarly to (*S*,*S*)-**18**, starting from alcohol **22** (0.1425 g, 0.5931 mmol), giving the product (0.1228 g, 0.4629 mmol, 78%) as a clear oil. $[\alpha]^{25}$ −34° (c = 0.25, $CHCl_3$); ^1H NMR (500 MHz, $CDCl_3$) δ (ppm) δ 7.44–7.30 (5H, m, ArH), 5.15 (2H, ABq, $\Delta\nu_{AB}$ = 4.98 Hz, J_{AB} = 12.3 Hz, $ArCH_2$), 4.69 (1H, dqd, J = 46.5, 6.3, 4.4 Hz, CHF), 3.57 (1H, dddd, J = 13.6, 10.4, 4.4, 3.3 Hz, CHN_3), 2.64–2.46 (2H, m, CH_2COO), 1.92 (1H, dtd, J = 14.2, 7.9, 3.3 Hz, CH_2CH_2COO), 1.67 (1H, dddd, J = 14.0, 10.4, 7.8, 5.7 Hz, CH_2CH_2COO), 1.39 (3H, dd, J = 24.4, 6.3 Hz, CH_3); ^{13}C NMR (126 MHz, $CDCl_3$) δ (ppm) 172.45, 135.65, 128.60, 128.36, 128.30, 91.66 (d, J = 172.8 Hz), 66.55, 64.64 (d, J = 21.4 Hz), 30.62, 24.82 (d, J = 6.0 Hz), 16.16 (d, J = 22.7 Hz); ^{19}F NMR (376 MHz, $CDCl_3$) δ (ppm) −177.12 (dqd, J = 45.9, 24.3, 13.5 Hz); ESI-MS (m/z, abundance): 223 (41, $[M-N_3]^+$).

4.2.19. (4*S*,5*R*)-4-Ammonio-5-fluorohexanoate (12)

This was synthesized by the same route as for compound (*S*,*S*)-**11**, using azido ester **23** (0.1063 g, 0.4007 mmol), and obtaining the product (23.2 mg, 0.156 mmol, 39%) as a white solid, mp 158–159 °C, $[\alpha]^{25}$ +15° (c = 0.24, CD_3OD); ^1H NMR (500 MHz, CD_3OD) δ (ppm) 4.98–4.81 (1H, m, CHF), 3.46–3.28 (1H, m, CHN), 2.57–2.33 (2H, m, CH_2COO), 2.01–1.69 (2H, m, CH_2CH_2COO), 1.42 (3H, dd, J = 24.2, 6.5 Hz, CH_3); ^{13}C NMR (126 MHz, CD_3OD) δ (ppm) 180.61, 90.97 (d, J = 171.2 Hz), 56.66 (d, J = 20.8 Hz), 35.81, 24.91 (d, J = 5.0 Hz), 16.00 (d, J = 22.4 Hz); ^{19}F NMR (376 MHz, CD_3OD) δ (ppm) −185.92 (1F, dqd, J = 47.8, 24.1, 19.3 Hz); HRMS (ESI) (m/z): 150.0925 (calcd for $C_6H_{13}FNO_2^+$: 150.0925, $[M+H]^+$); ee = 93% (from Mosher amide de); HPLC purity (retention time): 94% (0.794 min).

4.2.20. (4*R*,5*R*)-5-Fluoro-4-((*S*)-3,3,3-trifluoro-2-methoxy-2-phenylpropanamido)hexanoic acid

This compound was prepared exactly as the derivative of product (*S*,*S*)-**11**, but using amine **12** (6.1 mg, 41 μmol) and giving the product (13.6 mg, 37.3 μmol, 91%) as a clear oil, contaminated with (*S*)-Mosher's acid (2.7 mg, 11.3 μmol); $[\alpha]^{25}$ −17° (c = 0.96, $CHCl_3$), Corrected for Mosher's acid: $[\alpha]^{25}$ −1.0° (c = 0.80, $CHCl_3$); ^1H NMR (500 MHz, $CDCl_3$) δ (ppm) 7.56–7.46 (2H, m, ArH), 7.46–7.36 (3H, m, ArH), 7.03 (1H, d, J = 9.6 Hz, NH), 4.73 (1H, dqd, J = 48.4, 6.5, 3.5 Hz, CHF), 4.10 (1H, dddt, J = 24.1, 11.2, 9.7, 3.4 Hz, CHNH), 3.57 (1H, br s, COOH), 3.46 (3H, q, J = 1.6 Hz, OCH_3), 2.41–2.22 (2H, m, CH_2COOH), 2.08 (1H, dtd, J = 15.1, 7.7, 3.3 Hz, CH_2CH_2COOH), 1.75 (1H, dddd, J = 13.9, 11.2, 7.4, 6.0 Hz, CH_2CH_2COOH), 1.39 (3H, dd, J = 24.1, 6.4 Hz, $CHFCH_3$); ^{13}C NMR (126 MHz, $CDCl_3$) δ (ppm) 178.30, 166.70, 132.33, 129.63, 128.65, 127.33, 123.58 (q, J = 290.2 Hz), 91.83 (d, J = 171.6 Hz), 83.98 (q, J = 26.4 Hz), 55.02, 52.28 (d, J = 20.7 Hz), 30.00, 22.51 (d, J = 4.4 Hz), 17.41 (d, J = 22.2 Hz); ^{19}F NMR (376 MHz, $CDCl_3$) δ (ppm) −69.20 (3F, s, CF_3), −188.75 (1F, dp, J = 48.2, 24.0 Hz, CHF); de = 93% based on CF_3 peak (3.00 F at −69.20 ppm vs 0.11 F at −69.30 ppm); (ESI-MS (m/z, abundance): 729 (100, $[2M-H]^-$), 364 (12, $[M-H]^-$).

4.3. Computational methods

Renderings were performed in PyMOL.[16] Docking was performed either with Autodock[17,18] or Surflex-Dock.[19] The protein was downloaded from the Protein Data Bank (ID No. 1OHW)[14] and was prepared in SYBYL[20] by fixing all incomplete sidechains, and setting histidine, asparagine, glutamine, aspartate and glutamate protonation states and orientations. End caps were set to acetamides and *N*-methyl amides for the N- and C-termini, respectively, and hydrogen atoms were added. Only one set of dimers was used in this work. The structure of vigabatrin with PLP was extracted, and all extraneous molecules except waters were removed.

Waters were protonated so as to maximize polar contacts. Finally, Gasteiger-Marsili charges were calculated for all atoms.

Preparation of the structures for Autodock was further carried out using AutoDock Tools. All non-polar hydrogens were merged with their corresponding heavy atoms. During docking, several binding site sidechains were set as flexible: I72, E270, K329, Y348, F351 and T353. A binding site of 15 Å around the center of the vigabatrin–PLP complex was considered.

For Surflex-Dock, the protomol was generated from the prepared structure, and docking was carried out using the vigabatrin/PLP complex as a template. The same 15 Å radius was used, and the structures obtained were the best out of 100 docking poses.

The structures of the ligands in the GABA-AT active site were refined by molecular mechanics, using the GROMACS program.[21] Amber99 Force field parameters for the GABA-AT dimer were obtained with the pdb2gmx module, with parameters for the central FeS cluster derived from an ab initio calculation (NWChem, HF//6–31G*).[22] The protein was solvated in a dodecahedron-shaped box with 1 nm clearance on each side, and some waters were replaced with sodium and chloride ions, to give an effective concentration of 0.14 M (with adjustments to obtain a neutral system).

Parameters for the ligands and other organic molecules were obtained using the R.E.D. server[23] and transformed into topology files using the Antechamber module of the AMBER program.[24]

Because the simulations involved a protein dimer, one of the active sites was occupied with the desired ligands, while the other one included a molecule of PLP covalently bound to Lys329, and an acetate ion forming an ionic interaction with Arg192. These structures were obtained from the corresponding ligand-free entry in the Protein Data Bank (#1OHV).[14]

After the molecules were in the active site, the system was energy minimized, and molecular dynamics simulations ensued. The system was slowly warmed to 300 K (200 ns each at 100, 200, and 300 K), using position restraints (1000 kJ mol^{-1} nm^{-2}). After this time, the position restraints were removed, and the simulations were continued for 4 ns. After a final energy minimization, the structures were used for evaluation.

4.4. Enzymatic assays

GABA-AT was purified from fresh pig brains following the previously published procedure,[25] and was obtained with a concentration of 0.294 mg/mL and a specific activity of 1.74 units/mg. The behavior of the isolated GABA-AT was similar to that observed previously, with a K_m for GABA of 2.2 ± 0.4 mM, and a V_{max} of $(6.1 \pm 0.5) \times 10^{-6}$ mol L^{-1} min^{-1}.

Assay solutions consisted of 87 mM potassium pyrophosphate buffer (pH 8.6), with 6 mM GABA, 5 mM α-ketoglutaric acid, 1.25 mM $NADP^+$, and 3.3 mM β-mercaptoethanol. Enzyme activity was measured through the change in absorbance at 340 nM, corresponding to the transformation of $NADP^+$ to NADPH, based on the coupled assay of Scott and Jakoby.[26] The reactions were carried out in the presence of excess succinic semialdehyde dehydrogenase (SSADH), obtained from commercially available GABase (Sigma–Aldrich) by published methods.[27]

The inactivation (time-dependent inhibition) studies were performed as follows: GABA-AT (20 μL in 100 mM potassium phosphate buffer, pH 7.0, with 1 mM β-mercaptoethanol) was incubated at 25 °C with β-mercaptoethanol (1.25 μL of 100 mM solution), α-ketoglutaric acid (1.25 μL of 100 mM solution), and the tested compounds (2.5 μL of 50 mM solution for a final concentration of 5 mM). At different time points, 4 μL of this incubation mixture were transferred to a 96-well plate with 150 μL assay solution and excess SSADH, and activity (reaction rate) was measured in a Biotek Synergy H1 plate reader.

The reversible inhibition studies were carried out following a different sequence: The enzyme and SSADH were mixed with a solution containing 6.2 μL of inhibitor solution (at different concentrations) and 133.8 μL of assay solution; this mixture was measured directly for activity, as before. IC_{50} values were calculated using GraphPad PRISM version 5.0c for Mac OS X, GraphPad Software, San Diego, CA, USA, www.graphpad.com. K_i values were calculated using the Cheng–Prusoff equation. Graphs were replotted in Microsoft Excel 2010 for publication. Finally, the possibility of **11** and **12** undergoing metabolism and activating SSDH similar to GABA and succinic semialdehyde was ruled out; no NADPH production was observed in the absence of GABA.

Substrate activity assays were performed by measuring glutamate production by GABA-AT in the presence of the test compounds. After turnover of a substrate molecule, PLP is regenerated from PMP by transforming α-ketoglutarate to glutamate. The detection of glutamate was carried out using a non-amplified version of Invitrogen's Amplex® Red glutamate detection kit. In a 96-well plate, each well contained 0.5 μL GABA-AT, 0.8 μL glutamate oxidase (5 units/mL), 0.125 μL horseradish peroxidase (100 units/mL), 0.5 μL Amplex® Red solution (10 mM), 6 μL α-ketoglutarate (100 mM), and 3 μL of substrate (100 mM) in 89.1 μL 100 mM potassium pyrophosphate buffer (pH 8.6), for a total of 100 μL. Fluorescence was measured at 590 nm, with excitation at 530 nm. A glutamate standard curve was created with concentrations of 0, 2, 4, 6, 8, and 10 μM (with 20 min preincubation), and all the wells in the plate were scaled to the 10 μM standard (at 50,000 RFU, or reference fluorescence units). The highest rates of glutamate production, which occurred between 15 and 25 min of reaction time, were used for analysis.

Acknowledgments

The authors are grateful to the National Institutes of Health (GM066132 and DA030604) for financial support of this research and to Amit Walia for assistance in determining the purity of the final compounds.

References and notes

1. Tolman, J. A.; Faulkner, M. A. *Expert Opin. Pharmacother.* **2009**, *10*, 3077.
2. Nanavati, S. M.; Silverman, R. B. *J. Am. Chem. Soc.* **1991**, *113*, 9341.
3. Gardner, E. L.; Schiffer, W. K.; Horan, B. A.; Highfield, D.; Dewey, S. L.; Brodie, J. D., ; Ashby, C. R., Jr. *Synapse* **2002**, *46*, 240.
4. DeMarco, A.; Dalal, R. M.; Pai, J.; Aquilina, S. D.; Mullapudi, U.; Hammel, C.; Kothari, S. K.; Kahanda, M.; Liebling, C. N.; Patel, V.; Schiffer, W. K.; Brodie, J. D.; Dewey, S. L. *Synapse* **2009**, *63*, 87.
5. Paul, M.; Dewey, S. L.; Gardner, E. L.; Brodie, J. D.; Ashby, C. R., Jr. *Synapse* **2001**, *41*, 219.
6. Silverman, R. B.; Invergo, B. J. *Biochemistry* **1986**, *25*, 6817.
7. Silverman, R. B.; Muztar, A. J.; Levy, M. A.; Hirsch, J. D. *Life Sci.* **1983**, *32*, 2717.
8. Neal, M. J.; Shah, M. A. *Br. J. Pharmacol.* **1990**, *100*, 324.
9. Okumura, H.; Omote, M.; Takeshita, S. *Arzneimittel-Forschung* **1996**, *46*, 459.
10. Adachi, Y.; Kamei, N.; Yokoshima, S.; Fukuyama, T. *Org. Lett.* **2011**, *13*, 4446.
11. Bourque, E.; Kocienski, P. J.; Stocks, M.; Yuen, J. *Synthesis* **2005**, 3219.
12. Sammakia, T.; Jacobs, J. S. *Tetrahedron Lett.* **1999**, *40*, 2685.
13. Qiu, J.; Pingsterhaus, J. M.; Silverman, R. B. *J. Med. Chem.* **1999**, *42*, 4725.
14. Storici, P.; De Biase, D.; Bossa, F.; Bruno, S.; Mozzarelli, A.; Peneff, C.; Silverman, R. B.; Schirmer, T. *J. Biol. Chem.* **2004**, *279*, 363.
15. Sharpless, K. B.; Amberg, W.; Bennani, Y. L.; Crispino, G. A.; Hartung, J.; Jeong, K. S.; Kwong, H. L.; Morikawa, K.; Wang, Z. M. *J. Org. Chem.* **1992**, *57*, 2768.
16. The PyMOL Molecular Graphics System, Version 1.4.1. Schrödinger, LLC.
17. Huey, R.; Morris, G. M.; Olson, A. J.; Goodsell, D. S. *J. Comput. Chem.* **2007**, *28*, 1145.
18. Morris, G. M.; Huey, R.; Lindstrom, W.; Sanner, M. F.; Belew, R. K.; Goodsell, D. S.; Olson, A. J. *J. Comput. Chem.* **2009**, *30*, 2785.
19. Jain, A. N. *J. Comput. Aided Mol. Des.* **2007**, *21*, 281.
20. SYBYL 8.0, Tripos International, 1699 South Hanley Rd., St. Louis, MO 63144, USA.
21. Hess, B.; Kutzner, C.; van der Spoel, D.; Lindahl, E. *J. Chem. Theory Comput.* **2008**, *4*, 435.
22. Valiev, M.; Bylaska, E. J.; Govind, N.; Kowalski, K.; Straatsma, T. P.; Van Dam, H. J. J.; Wang, D.; Nieplocha, J.; Apra, E.; Windus, T. L.; de Jong, W. *Comput. Phys. Commun.* **2010**, *181*, 1477.

23. Vanquelef, E.; Simon, S.; Marquant, G.; Garcia, E.; Klimerak, G.; Delepine, J. C.; Cieplak, P.; Dupradeau, F. Y. *Nucleic Acids Res.* **2011**, *39*, W511.
24. Wang, J. M.; Wang, W.; Kollman, P. A.; Case, D. A. *J. Mol. Graph. Model.* **2006**, *25*, 247.
25. Churchich, J. E.; Moses, U. *J. Biol. Chem.* **1981**, *256*, 1101.
26. Scott, E. M.; Jakoby, W. B. *J. Biol. Chem.* **1959**, *234*, 932.
27. Jeffery, D.; Weitzman, P. D. J.; Lunt, G. G. *Insect Biochem.* **1988**, *18*, 347.